ORGANOMETALLICS

Article

pubs.acs.org/Organometallics

Oxygen Atom Insertion into Iron(II) Phenyl and Methyl Bonds: A Key Step for Catalytic Hydrocarbon Functionalization

Jiajun Mei,[†] Daniel B. Pardue,[‡] Steven E. Kalman,[†] T. Brent Gunnoe,[*,†] Thomas R. Cundari,[*,‡] and Michal Sabat[§]

[†]Department of Chemistry and [§]Nanoscale Materials Characterization Facility, Materials Science and Engineering Department, University of Virginia, Charlottesville, Virginia 22904, United States

[‡]Department of Chemistry and Center for Advanced Scientific Computing and Modeling, University of North Texas, Denton, Texas 76203, United States

Ⓢ *Supporting Information*

ABSTRACT: Oxy-functionalization of metal−alkyl and −aryl bonds is a key step in potential hydrocarbon oxidation catalysis. However, well-defined examples of M−R to ROH conversion are rare, especially for first-row transition metals. Cp*Fe(CO)(NCMe)Ph reacts with oxygen or hydrogen peroxide to produce benzoic acid. Removing CO from the Cp*Fe(L)(L′)Ph framework allows simple oxygen atom insertion into the Fe−Ph bond. Cp*Fe($P(OCH_2)_3CEt$)$_2$Ph reacts with Me_3NO in THF to produce PhOH in high yield when Brønsted acids are added. Studies show that light promotes $P(OCH_2)_3CEt$ dissociation from Cp*Fe($P(OCH_2)_3CEt$)$_2$Ph, which facilitates the conversion to PhOH. The methyl analogue Cp*Fe[$P(OCH_2)_3CEt$]$_2$Me reacts with oxidants to produce MeOH.

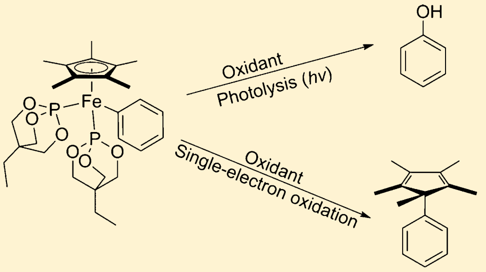

INTRODUCTION

The selective catalytic oxidation of hydrocarbons is an important but challenging process.[1−14] Enzymes perform C−H oxidation via high-valent Fe−oxo complexes, which initiate net H-atom abstraction to generate a transient radical.[15−17] A C−O bond forming "rebound" step followed by alcohol dissociation completes the conversion.[18] While progress has been made using synthetic metal−oxo complexes that initiate H atom abstraction,[15,19−24] successful extension to substrates possessing C−H bond dissociation enthalpies of >100 kcal/mol (e.g., light alkanes or arenes) is challenging.[19−22] In contrast, transition metal mediated C−H activation, defined herein as a process where the C−H bond coordinates to the metal before being broken, often affords activation of C−H bonds with bond dissociation energies of >100 kcal/mol.[5−7,12,13,25−32]

One strategy for metal-mediated C−O bond formation involves net oxygen atom insertion into metal−alkyl bonds (Scheme 1), which can occur via a metal−oxo intermediate or a Baeyer−Villiger-type pathway.[6,33−36] The Baeyer−Villiger pathway involves concerted C−O bond formation with Y−O bond breaking (Scheme 1). Since the activation of C−H bonds via 1,2-addition across M−X (X = OR, NR, NR_2) bonds has been reported,[30,33,37−42] the development of catalytic cycles is potentially viable (Scheme 1). Insertions of oxygen atoms into M−C bonds via nonradical routes are rare, and the majority of examples involve high valent d^0 metals that are incapable of C−H activation.[33,34,43−47] To our knowledge, O-atom insertion into M−R bonds for non-d^0 metals includes only Ni(II), Pd(II), and one example of a two-coordinate Fe(II) complex.[45,48−50]

Scheme 1. Proposed Pathways for Partial Oxidation of Hydrocarbons Involving Oxygen Atom Insertion into a M−R Bond and 1,2-CH-Addition across a M−OR Bond

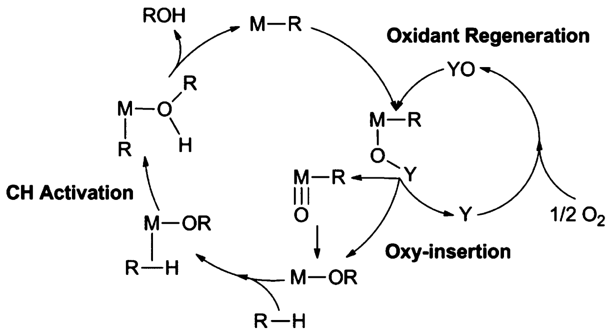

We recently reported facile C−H activation by Cp*Fe(CO)(NCMe)Ph (Cp* = 1,2,3,4,5-pentamethylcyclopentadienyl).[51] Having observed C−H activation, Cp*Fe(L)(L′)Ph complexes were deemed a good starting point to pursue Fe-mediated C−O bond formation. A computational study of metal-mediated C−O bond formation by Cp*Fe(CO)(NCMe)R (R = Me or Ph) indicated that O-atom insertion to form Fe−OR should be kinetically feasible.[52] Consistent with the prediction based on theory, herein is reported the observation of conversion of Fe−R bonds and oxidants into alcohols.

Received: September 3, 2014
Published: September 18, 2014

RESULTS AND DISCUSSION

The reaction of Cp*Fe(CO)(NCMe)Ph (**1**) with various oxidants results in either decomposition or the production of benzoic acid (eq 1 and Table 1). For some oxidants, the Cp* ligand is oxidized to 1,2,3,4-tetramethylfulvene (Table 1, entries 1−6). Benzene is formed in many cases (Table 1, entries 1−3 and 5−8), which is presumed to result from protonation (protic oxidants) and/or Fe−Ph bond homolysis from an oxidized intermediate [likely Fe(III)].[53] Although previous calculations showed that the formation of Cp*Fe(CO)(NCMe)OPh from reaction of Cp*Fe(CO)(NCMe)Ph and pyridine *N*-oxide should be kinetically accessible,[52] CO insertion into the Fe−Ph bond competes with O-atom insertion. Consistent with this suggestion, a computational study predicts a $\Delta G^{\ddagger}$ of 12.7 kcal/mol for CO insertion into the Fe−Ph bond of Cp*Fe(CO)(NCMe)Ph (Scheme 2). In contrast, the overall calculated $\Delta G^{\ddagger}$ for conversion of Cp*Fe(CO)(NCMe)Ph and pyridine *N*-oxide to Cp*Fe(CO)(OPh) is approximately 33.1 kcal/mol. Because of the competition of CO insertion, the reactivity with a Cp*Fe(L)$_2$R complex without a CO coligand was probed.

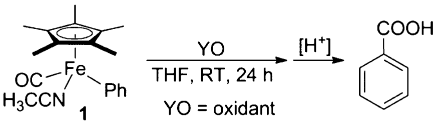

(1)

Table 1. Reaction Conditions, Products, and Yields for the Reactions of Cp*Fe(CO)(NCMe)Ph (1) with Various Oxidants[a]

no.	oxidant	*T* (°C)	*t* (h)	PhCOOH (%)[b]	benzene (%)	fulvene[c] (%)
1	O_2 (15 psi)	21	24	60	20	>90
2	Me_3NO	21	0.5	0	>90	>90
3	PyO	60	24	0	10	10
4	PyO	hν	1.5	0	0	15
5	mCPBA	21	0.5	0	>90	<10
6	$^nBu_4NIO_4$	21	0.5	10	10	>90
7	H_2O_2	21	0.5	60	<10	0
8	^tBuOOH	21	24	0	90	0

[a] Reactions are with 3 equiv of oxidant in THF-d_8 in NMR tubes. [b] Yields of products are based on integration of ^1H NMR spectra versus an internal standard. [c] Fulvene = 1,2,3,4-tetramethylfulvene.

The reaction of [(TMEDA)FeCl$_2$]$_n$ (n = 1, 2) (TMEDA = *N,N,N′,N′*-tetramethylethylenediamine) with P(OCH$_2$)$_3$CEt and Cp*Li produces Cp*Fe[P(OCH$_2$)$_3$CEt]$_2$Cl (**2**) in 70% isolated yield. Complex **2** reacts with PhLi to give Cp*Fe(P(OCH$_2$)$_3$CEt)$_2$Ph (**3**) in 62% isolated yield (Scheme 3). Complex **3** was characterized by single-crystal X-ray diffraction (Scheme 3).

Under ambient light, monitoring the reaction of Cp*Fe(P(OCH$_2$)$_3$CEt)$_2$Ph (**3**) with excess Me$_3$NO in THF-d_8 by ^1H NMR spectroscopy reveals the transformation of **3** to several products after 4 days at room temperature. The addition of Brønsted acid (e.g., H$_2$O or HCl) results in the production of PhOH in 70% yield (^1H NMR) relative to **3**. Phenol production has been confirmed by ^1H NMR spectroscopy and GC-MS. The control reaction of **3** and water (THF-d_8, room temperature) produces benzene without observation of phenol. During the reaction of **3** with Me$_3$NO, prior to addition of acid, the phenyl ligand of **3** is converted to a new species that has been identified as PhOH·ONMe$_3$ (see Experimental Section and Supporting Information).

For the reaction of **3** with Me$_3$NO, in addition to PhOH production, the Cp* ligand is oxidized to 1,2,3,4-tetramethylfulvene and the phosphite ligands are oxidized to phosphate,

Scheme 2. Calculated Free Energies for the Reaction of Cp*Fe(CO)(NCMe)Ph (1) and Pyridine *N*-oxide (PyO) in THF-d_8[a]

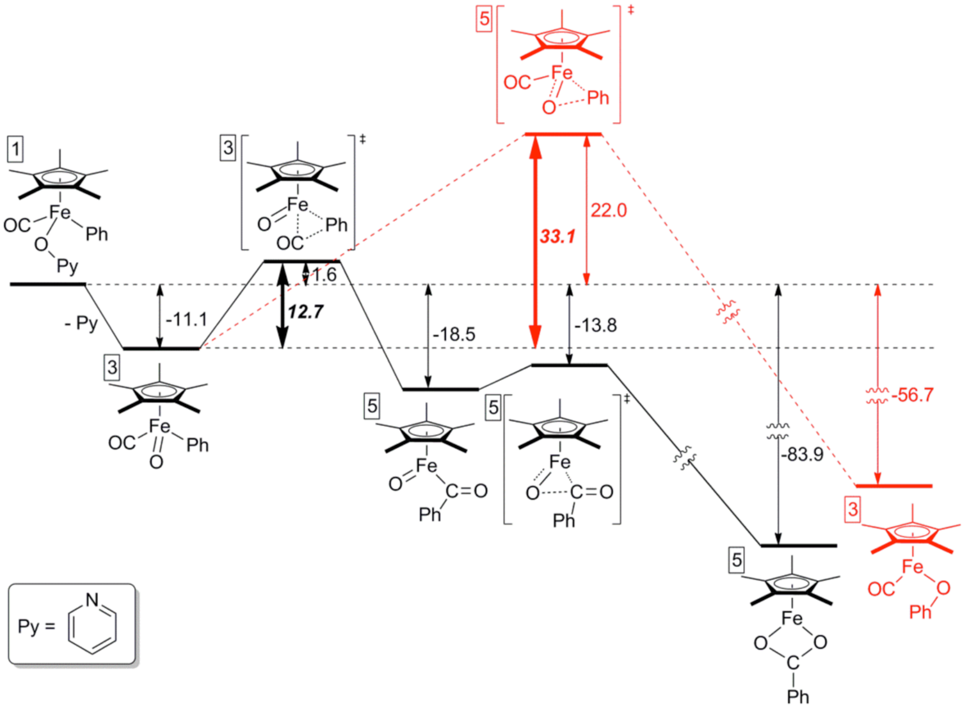

[a] Numbers are free energies (kcal/mol) relative to Cp*Fe(CO)(ONMe$_3$)Ph. Lowest energy spin states are labeled in the boxes on the top left of structures.

Scheme 3. Synthesis of $Cp^*Fe(P(OCH_2)_3CEt)_2Ph$ (3)[a]

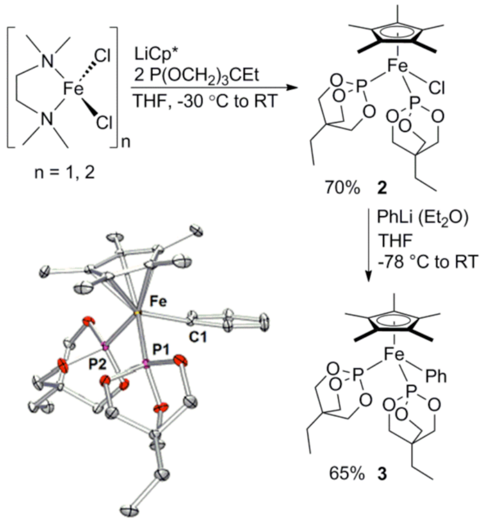

[a]ORTEP drawing of 3 (50% probability ellipsoids; H atoms omitted). Selected bond lengths (Å): Fe−C1 1.9993(2), Fe−P1 2.0854(4), Fe−P2 2.0996(4). Selected bond angles (deg): C1−Fe−P1 92.91(4), C1−Fe−P2 92.73(4), P1−Fe−P2 91.65(2).

as indicated by a resonance in the ^{31}P NMR spectrum at −8.2 ppm.[54] A brown precipitate is also observed, but we have been unable to characterize this material. Thus, the reaction of **3** and Me_3NO results in the oxidation of Cp*, both $P(OCH_2)_3CEt$ ligands, and the phenyl ligand (eq 2). When **3** is treated with only 1 equiv of Me_3NO, partial conversion of **3** to the same products occurs.

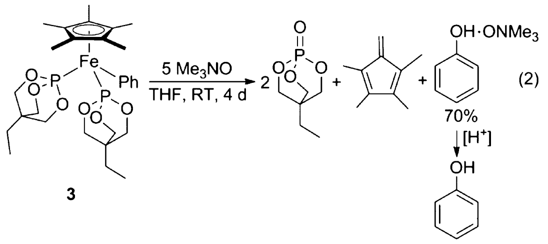

No reaction is observed for **3** and Me_3NO after 1 week in the absence of light even upon heating at 80 °C. When photolyzed, the reaction of **3** and Me_3NO is complete within 2 h to produce $PhOH{\cdot}ONMe_3$ (compared to 4 days in ambient light). The addition of Brønsted acid (e.g., H_2O or HCl) to the reaction mixture results in the formation of PhOH (eq 3). Further studies showed that light is required for dissociation of a phosphite ligand (see below) in the conversion of **3** and Me_3NO.

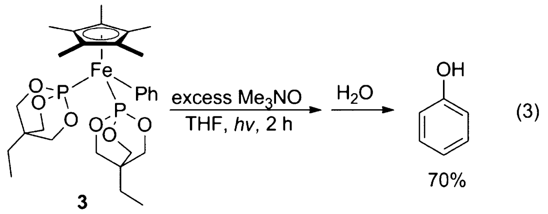

We first considered a radical pathway for the net oxygen atom insertion into the Fe−Ph bond. However, no significant change in the product or rate is observed when the same reaction is performed in the presence of radical traps such as TEMPO [(2,2,6,6-tetramethylpiperidin-1-yl)oxyl] or 1,4-cyclohexadiene. Since TEMPO is known to trap phenyl radical,[55] this suggests that free phenyl radical is not formed in the reaction of **3** with Me_3NO. However, these experiments cannot rule out a short-lived phenyl radical that rapidly recombines with an Fe−O moiety. We also considered a pathway involving decomposition of complex **3** in the presence of light to form an unobserved Fe catalyst (e.g., Fe nanoparticles), which then catalyzes the oxidation of benzene to phenol. Complex **3** and excess Me_3NO were reacted in the presence of excess benzene, but the catalytic conversion of benzene to phenol was not observed. We also performed this reaction in the presence of excess 1,4-cyclohexadiene (to provide a source of hydrogen) and, again, did not observe catalytic production of PhOH. Thus, if an *in situ* Fe catalyst for benzene oxidation is formed, it is limited to <1 turnover. While they do not definitively eliminate *in situ* formation of an Fe catalyst from consideration, these experimental results are most consistent with a stoichiometric oxidation reaction.

It was hypothesized that light might promote $P(OCH_2)_3CEt$ dissociation from **3**. In the dark, there is no reaction between complex **3** and excess PMe_3 (THF-d_8) after 1 week at 80 °C. In contrast, complex **3** is quantitatively converted to $Cp^*Fe(P(OCH_2)_3CEt)(PMe_3)Ph$ (**4**) within 2 h under photolysis at room temperature (eq 4). Under pseudo-first-order conditions (i.e., excess PMe_3), complex **2** was treated with a series of concentrations of PMe_3 in THF-d_8 under photolysis, and a first-order rate constant for the disappearance of complex **3** was determined for each reaction. Within deviation of the data, a plot of k_{obs} as a function of $[PMe_3]$ shows a zero-order dependence on $[PMe_3]$ (Figure 1). The average k_{obs} value is $0.8(3) \times 10^{-3}$ s^{-1}. The large deviations in k_{obs} are a result of challenges associated with reproducibility using the photolysis lamp (e.g., rate changes as a function of distance from the lamp). As expected for an 18-electron complex, the kinetic data are consistent with a dissociative ligand exchange with $P(OCH_2)_3CEt$ dissociation as the rate-limiting step.

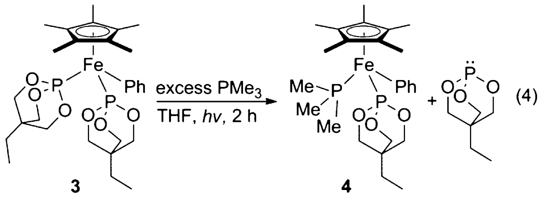

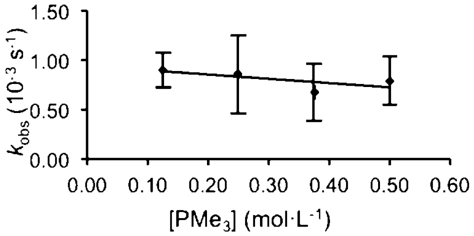

Figure 1. Plot of k_{obs} vs $[PMe_3]$ for the reaction of $Cp^*Fe(P(OCH_2)_3CEt)_2Ph$ (**3**) with PMe_3 showing a zero-order dependence on $[PMe_3]$.

The reaction of **3** and Me_3NO in THF-d_8 was monitored by ^1H and ^{31}P NMR spectroscopy under the same photolysis conditions as the reaction of **3** and PMe_3. Free $P(OCH_2)_3CEt$ is formed and then converted to $O{=}P(OCH_2)_3CEt$, which

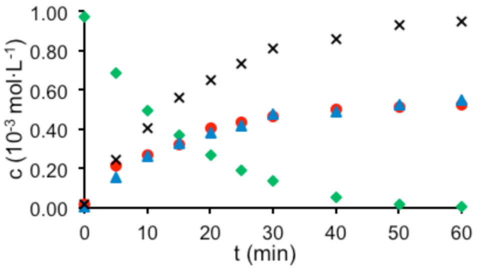

Figure 2. Plot of concentration versus time for the starting material and three products observed during the reaction of Cp*Fe(P(OCH$_2$)$_3$CEt)$_2$Ph (**3**) with Me$_3$NO in THF-d_8 including complex **3** (green, diamonds), O═P(OCH$_2$)$_3$CEt (black, ×), 1,2,3,4-tetramethylfulvene (blue, triangles), and PhOH·ONMe$_3$ (red, circles).

supports dissociation of P(OCH$_2$)$_3$CEt under photolysis as the first step of oxygen atom insertion into the Fe−Ph bond.

Figure 2 depicts the concentration versus time plot for the starting material **3** and the three products shown in eq 2 (based on the integrations of ^{1}H NMR spectra). Since oxidation of free P(OCH$_2$)$_3$CEt by Me$_3$NO occurs in the absence of photolysis, we did not monitor the concentration of free P(OCH$_2$)$_3$CEt. In the plot, in order to keep the *y*-scale similar for all compounds, the concentration of O═P(OCH$_2$)$_3$CEt is divided by 2. Using a first-order fit for the disappearance of **3** gave k_{obs} = 1.0(1) × 10^{-3} s^{-1}, which is almost identical to the k_{obs} for phosphite/PMe$_3$ exchange (see above). This is consistent with rate-limiting phosphite dissociation for the formation of PhOH. The generation of PhOH·ONMe$_3$ and 1,2,3,4-tetramethylfulvene have almost identical rates with a k_{obs} = 0.9(1) × 10^{-3} s^{-1} as the decay of **3**. The oxidation of free P(OCH$_2$)$_3$CEt with Me$_3$NO (under the same pseudo-first-order conditions) in THF-d_8 was independently determined by ^{1}H NMR spectroscopy at room temperature, and k_{obs} = 0.55(1) × 10^{-3} s^{-1} was determined (Figure 3), which is consistent with the observation of a low concentration of free phosphite that is ultimately converted to phosphate. The plot in Figure 2 shows no evidence of an induction period.

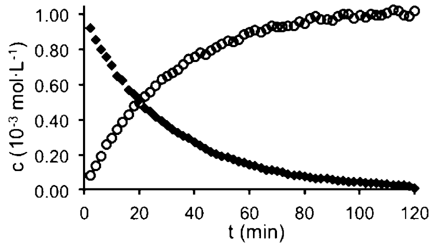

Figure 3. Plot of concentration versus time for the reaction of P(OCH$_2$)$_3$CEt with Me$_3$NO in THF-d_8 to produce O═P(OCH$_2$)$_3$CEt. [P(OCH$_2$)$_3$CEt (diamonds), O═P(OCH$_2$)$_3$CEt (circles)].

Previous computational studies of O-atom insertion into the Fe−R bonds of Cp*Fe(CO)(NCMe)R from reactions with oxidants revealed that the most favorable pathway would likely involve formation of the Fe−oxo intermediate Cp*Fe(CO)(O)R followed by migratory insertion of the hydrocarbyl ligand to the oxo ligand.[52] We extended the computational studies to Cp*Fe(P(OCH$_2$)$_3$CEt)$_2$Ph with the assumption that the analogous Fe−oxo complex, Cp*Fe(P(OCH$_2$)$_3$CEt)(O)Ph, is an intermediate. Density functional theory (DFT) calculations were carried out to determine the energy barriers for the three observed oxidation reactions following the dissociation of the P(OCH$_2$)$_3$CEt and the formation of the Fe═O intermediate: the oxidation of coordinated P(OCH$_2$)$_3$CEt to form O═P(OCH$_2$)$_3$CEt, conversion of Ph−Fe═O to form Fe−OPh, and oxidation of Cp* to form 1,2,3,4-tetramethylfulvene (Scheme 4).

Complex **3** is calculated to possess a singlet spin ground state. Fe remains bonded to Cp* in an η^5 fashion throughout the reaction coordinate. Overall, the oxy-insertion product Cp*Fe(P(OCH$_2$)$_3$CEt)(OPh) is calculated to be highly exergonic relative to the starting materials (ΔG = −65.4 kcal/mol). Upon dissociation of the phosphite ligand from **3**, which is found to be endergonic by 1.7 kcal/mol, a spin flip from the singlet to a triplet occurs. The minimum energy crossing point (MECP) for phosphine loss was calculated using Harvey's method.[56,57] The singlet → triplet "spin flip" associated with phosphite dissociation was calculated to be energetically demanding, lying ~20 kcal/mol above complex **3**, and hence engendering a barrier that is similar to the OAT barrier (*vide infra*) and consistent with the experimental proposal of rate-determining phosphite dissociation.

Coordination of Me$_3$NO to Cp*Fe(P(OCH$_2$)$_3$CEt)Ph was calculated to stabilize the complex by 2.2 kcal/mol with ΔG = 0.5 kcal/mol compared to the starting complex **3**. Another spin flip (triplet → quintet) accompanies the transformation of Cp*Fe(P(OCH$_2$)$_3$CEt)Ph → Cp*Fe(P(OCH$_2$)$_3$CEt)(ONMe$_3$)Ph. Attempts to find phosphite/ONMe$_3$ ligand exchange via an associative mechanism were not successful, and thus, consistent with the kinetic study of P(OCH$_2$)$_3$CEt/PMe$_3$ exchange (see above), the simulations imply a dissociative mechanism.

Conversion of Cp*Fe(P(OCH$_2$)$_3$CEt)(ONMe$_3$)Ph to an Fe^{IV}−oxo Cp*Fe(P(OCH$_2$)$_3$CEt)(O)Ph is calculated to be exergonic (ΔG = −15.5 kcal/mol relative to **3**). The transition state for the oxygen atom transfer was calculated to be 20.0 kcal/mol above Cp*Fe(P(OCH$_2$)$_3$CEt)(ONMe$_3$)Ph with a quintet spin state. Formation of Cp*Fe(P(OCH$_2$)$_3$CEt)(O)Ph entails another spin flip to a triplet upon formation of the oxo intermediate. The Fe of Cp*Fe(P(OCH$_2$)$_3$CEt)(O)Ph has a spin density of 1.315 e^-, while the oxo has a 0.819 e^- spin density. This suggests the oxo intermediate possesses oxyl (O$^{-\bullet}$) character. The spin density plot can be seen in Figure 4, showing the alpha spin (orange) being shared between the oxyl and Fe while a small amount of beta spin (purple) is on the phenyl ligand.

Migration of the phenyl ligand to the Fe−oxo bond (Scheme 4, blue pathway) results in a calculated free energy barrier of 16.8 kcal/mol and was found to be exergonic by 65.4 kcal/mol upon formation of the quintet phenoxide product Cp*Fe(P(OCH$_2$)$_3$CEt)(OPh). Thus, the calculations predict that formation of the oxo complex occurs with a more substantial free energy of activation than the phenyl migration step. Similar to calculations of oxy-insertion into the Fe−Ph bond of Cp*Fe(CO)(NCMe)Ph,[52] the calculations predict that conversion of Cp*Fe(P(OCH$_2$)$_3$CEt)$_2$Ph and Me$_3$NO to Cp*Fe(P(OCH$_2$)$_3$CEt)(OPh) is kinetically feasible.

From the oxo complex Cp*Fe(P(OCH$_2$)$_3$CEt)(O)Ph, the phosphite can migrate to the oxo ligand to form phosphate (Scheme 4, black pathway). The calculated free energy barrier to form phosphate from Cp*Fe(P(OCH$_2$)$_3$CEt)(O)Ph is 11.8 kcal/mol. The formation of the phosphate product Cp*Fe(O═P(OCH$_2$)$_3$CEt)Ph is 13.8 kcal/mol exergonic in relation to the starting material Cp*Fe(P(OCH$_2$)$_3$CEt)$_2$Ph. These results suggest that phosphate formation can originate from Cp*Fe(P(OCH$_2$)$_3$CEt)(O)Ph or free phosphite (see above).

Scheme 4. Calculated Free Energies for the Reaction of Cp*Fe(P(OCH$_2$)$_3$CEt)$_2$Ph (3) and Me$_3$NO in THF-d_8^{a}

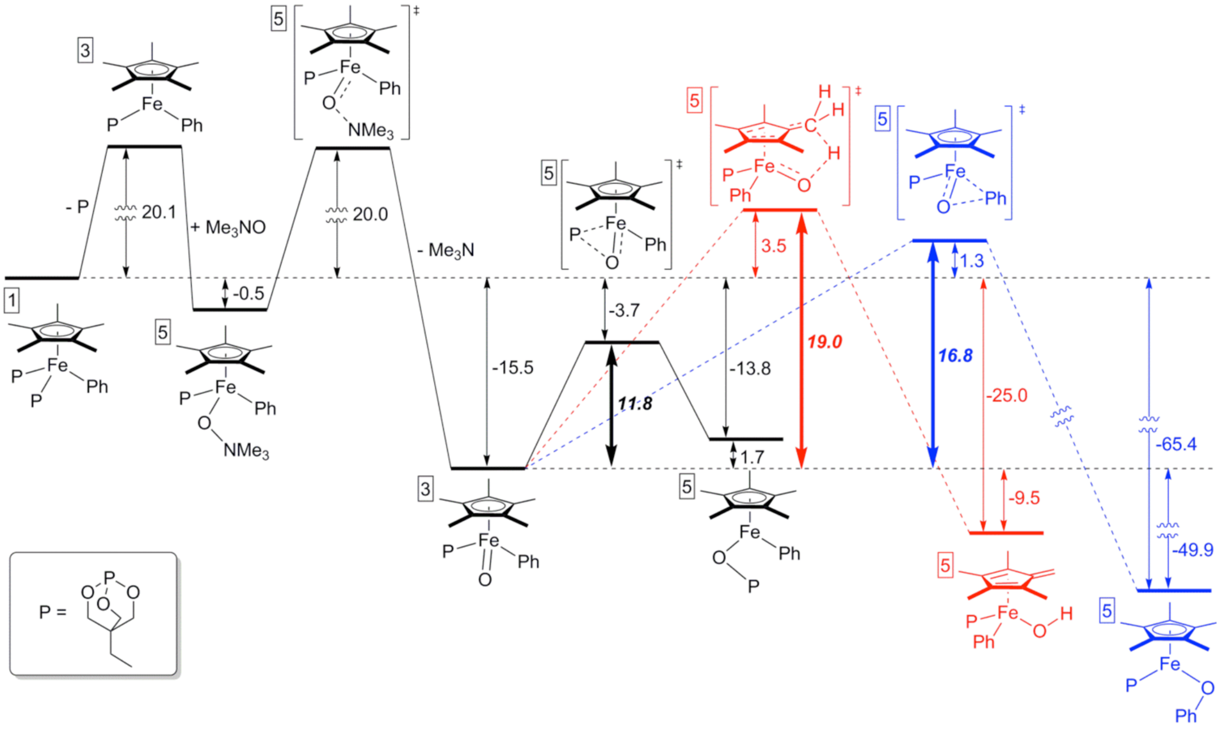

^{a}Numbers are free energies (kcal/mol) relative to complex **3**. Lowest energy spin states are labeled in the box on the top left of structures.

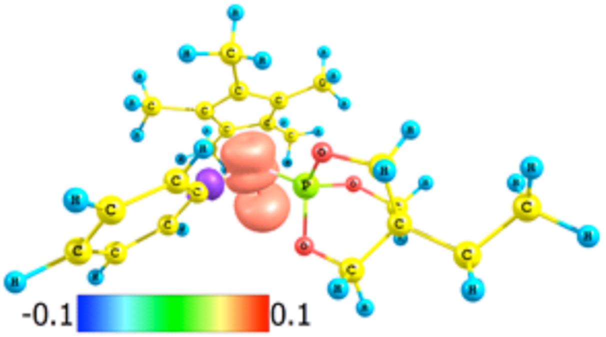

Figure 4. Spin density plot of oxo intermediate Cp*Fe(P(OCH$_2$)$_3$CEt)(O)Ph [scale: 0.33, contour value: 0.006 943].

Scheme 5. Proposed Pathway for the Reaction of Cp*Fe(P(OCH$_2$)$_3$CEt)$_2$Ph (3) and AgOTf

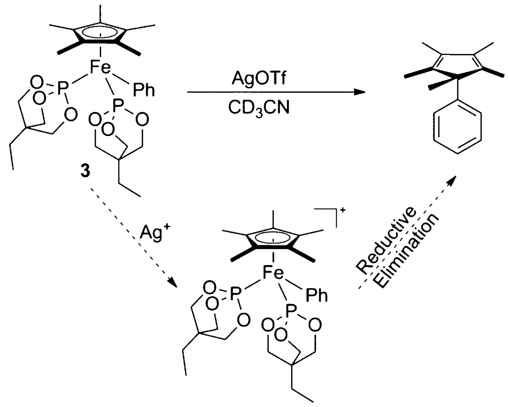

Oxidation of Cp* was also modeled computationally (Scheme 4, red pathway). From Cp*Fe(P(OCH$_2$)$_3$CEt)(O)Ph, the formation of 1,2,3,4-tetramethylfulvene via H-atom transfer to the oxo ligand was calculated to have a free energy barrier of 19.0 kcal/mol.

In contrast to the reaction of **3** with Me$_3$NO, the reaction of **3** with sodium periodate in a THF/H$_2$O mixture results in the quantitative production of 1,2,3,4,5-pentamethyl-5-phenylcyclopentadiene (Cp*Ph) after 24 h by ^{1}H NMR spectroscopy (eq 5). We considered that the formation of Cp*Ph might result from an initial electron transfer to form the Fe$^{\text{III}}$ complex [Cp*Fe(P(OCH$_2$)$_3$CEt)$_2$Ph]$^+$ followed by C−C reductive elimination. Consistent with this proposal, the reaction of **3** with AgOTf (OTf = trifluoromethanesulfonate), a known single-electron oxidant in darkness, results in the formation of Cp*Ph in quantitative yield (Scheme 5). DFT calculations reveal that the free energy barrier for the formation of Cp*Ph via direct C−C reductive elimination is 40.1 kcal/mol from Fe(II) complex **3**, but the calculated free energy barrier is reduced to 19.4 kcal/mol for the cationic, formally Fe(III) complex [Cp*Fe(P(OCH$_2$)$_3$CEt)$_2$Ph]$^+$ (Scheme 6).

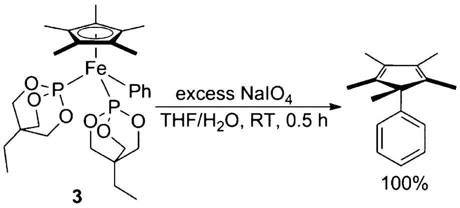

(5)

Table 2 shows the yields of PhOH and Cp*Ph for the reactions of **3** with a range of oxidants and solvents. The production of PhOH requires light (either ambient or photolysis lamp); however, Cp*Ph formation occurs in the absence of light. These observations are consistent with light-induced dissociation of phosphite as key step in the formation of PhOH but not Cp*Ph. Although *N*-oxides are not typically considered

Scheme 6. Calculated Free Energies for the Reaction of $Cp^*Fe(P(OCH_2)_3CEt)_2Ph$ (3) and AgOTf in THF-d_8[a]

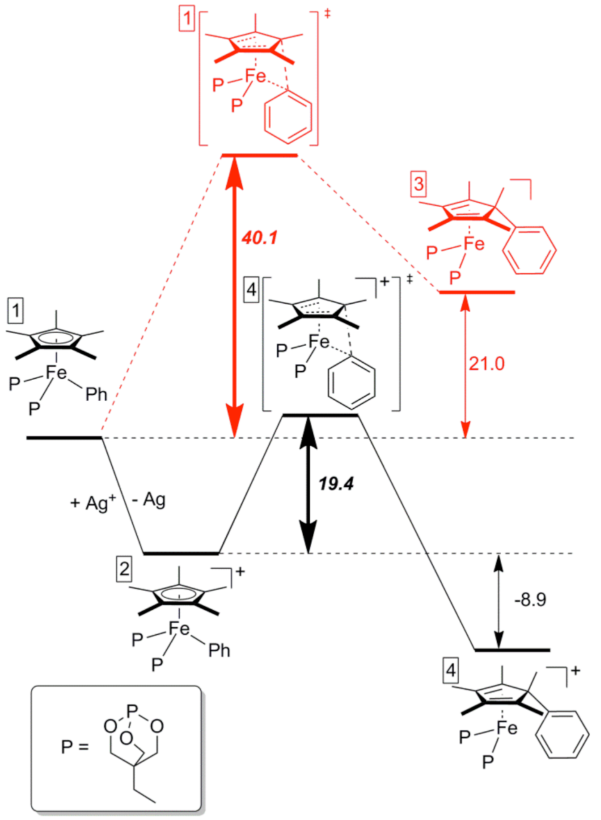

[a]Numbers are free energies (kcal/mol) relative to complex 3. Lowest energy spin states are labeled in the box on the top left of structures.

Table 2. Reaction Conditions and Yields for $Cp^*Fe(P(OCH_2)_3CEt)_2Ph$ (3) with Various Oxidants[a]

no.	oxidant	solvent	T (°C)[b]	t (h)	PhOH (%)[c]	Cp*Ph (%)
1	Me_3NO	THF	21	96	70	10
2	Me_3NO	THF	21 ($h\nu$)	2	70	10
3	Me_3NO	CH_3CN	21	96	0	80
4	NMO[d]	THF	21	72	70	10
5	O_2 (15 psi)	CH_3CN	21	24	0	90
6	O_2 (15 psi)	THF	21	24	15	20
7	O_2 (15 psi)	THF	21 ($h\nu$)	1	15	20
8	$^nBU_4NIO_4$	THF	21 ($h\nu$)	4	25	12
9	$NaIO_4$	THF/ H_2O	21	0.5	0	100
10	$^nBU_4NIO_4$	CH_3CN	21	24	0	90
11	H_2O_2	THF	21	72	10	80
12	H_2O_2	THF	21 ($h\nu$)	4	13	15
13	PyO	THF	21 ($h\nu$)	4	0	0
14	PyO	THF	70	96	0	70
15	4-NO_2-PyO	CH_3CN	50	24	0	90
16	AgOTf	CH_3CN	21	0.5	0	100

[a]Reactions incorporate 5 equiv of oxidant in deuterated solvents. [b]All reactions were performed under ambient or UV light. $h\nu$ is used to show reactions performed under UV light. PhOH is not observed when reactions are performed in the absence of light. [c]Yields of products are based on integration of ^1H NMR spectra versus an internal standard. [d]NMO = N-methylmorpholine N-oxide.

single-electron oxidants, such reactivity has precedent.[58] Complex **3** reacts with Me_3NO in THF to produce a high yield of PhOH under either photolysis or ambient light (entries 1 and 2), but only the C−C coupling product is observed in MeCN (entry 3). Although we do not have a definitive explanation for the solvent effect, it is possible the MeCN may promote electron transfer due to its polar nature by stabilizing incipient charge in the transition states for the formation of $[Cp^*Fe(P(OCH_2)_3CEt)_2Ph]^+$. Alternatively, MeCN might inhibit coordination of Me_3NO to Fe and suppress the oxy-insertion reaction, while the proposed mechanism for formation of Cp*Ph does not require a vacant coordination site on Fe. $^nBu_4NIO_4$ and H_2O_2 also generate PhOH in THF (Table 2, entries 8, 11, and 12). Aerobic oxidation of the Fe−Ph to form PhOH is also observed, although the yield is low (Table 2, entries 6 and 7). Taken together, these results suggest that PhOH formation does not likely occur by an initial single-electron transfer to generate an Fe(III) intermediate. Rather, the reaction is hypothesized to occur by initial $P(OCH_2)_3CEt/Me_3NO$ ligand exchange to generate $Cp^*Fe(P(OCH_2)_3CEt)(Me_3NO)Ph$, which then undergoes net O-atom transfer to the phenyl ligand.

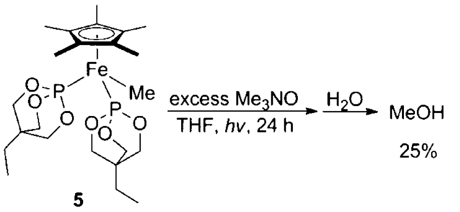

(6)

We have also prepared and isolated the methyl complex $Cp^*Fe(P(OCH_2)_3CEt)_2Me$ (**5**). When treated with Me_3NO in THF, complex **5** displays analogous reactivity to **3** to produce MeOH, but with a lower yield (~25%) by ^1H NMR spectroscopy (eq 6). The C−C reductive elimination product 1,2,3,4,5,5-hexamethylcyclopentadiene (Cp*Me) is also observed when **5** reacts with Me_3NO or O_2 in CD_3CN, with MeOH as the coproduct (eq 7). Table 3 shows the results of the reactions of **5** with various oxidants.

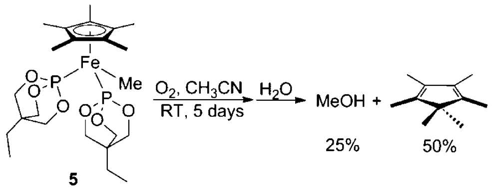

(7)

■ SUMMARY AND CONCLUSIONS

Insertion of oxygen atoms into metal−hydrocarbyl bonds is a key step in the development of potential catalysts for the oxidation of hydrocarbons as shown in Scheme 1. Despite the potential importance of such oxygen atom insertion reactions, there are few examples of nonradical conversion of M−R bonds and oxygen atom transfer reagents to M−OR. Herein, it is demonstrated that Fe(II) hydrocarbyl (phenyl and methyl) complexes undergo C−O bond formation upon reaction with certain oxidants. The experimental observations were augmented by computational studies that indicate Fe−oxo complexes as viable intermediates that precede net oxo insertion into the Fe−R bond. The reaction requires light, presumably to initiate ligand exchange between phosphite and the oxidant. The calculations indicate that both Fe−oxo formation and the oxy-insertion into Fe−R bonds are thermally viable processes. Although the previous (limited) examples of O-atom insertion into M−R

Table 3. Reaction Conditions and Yields for Reaction of Cp*Fe(P(OCH$_2$)$_3$CEt)$_2$Me (5) with Various Oxidants[a]

no.	oxidant	solvent	T (°C)	t (h)	MeOH (%)[b]	Cp*Me (%)
1	Me$_3$NO	THF	21	96	25	0
2	Me$_3$NO	THF	21 ($h\nu$)	24	25	0
3	Me$_3$NO	CH$_3$CN	21	96	25	0
4	NMO[c]	THF	21	96	25	0
5	O$_2$ (15 psi)	CH$_3$CN	21	24	0	90
6	O$_2$ (15 psi)	THF	21	24	16	70
7	O$_2$ (15 psi)	THF	21 ($h\nu$)	24	22	0
8	^{n}Bu$_4$NIO$_4$	THF	21 ($h\nu$)	4	10	0
9	NaIO$_4$	THF/ H$_2$O	21	0.5	0	100
10	^{n}Bu$_4$NIO$_4$	CH$_3$CN	21	24	0	83
11	H$_2$O$_2$	THF	21	24	26	0
12	H$_2$O$_2$	THF	21 ($h\nu$)	2	20	0
13	PyO	THF	21 ($h\nu$)	4	0	0
14	PyO	THF	70	96	0	70
15	4-NO$_2$-PyO	CH$_3$CN	50	24	0	76
16	AgOTf	CH$_3$CN	21	0.5	0	100

[a] Reactions are performed with 5 equiv of oxidant in deuterated solvents. [b] Yields of products are based on integration of ^{1}H NMR spectra versus an internal standard. [c] NMO = *N*-methylmorpholine *N*-oxide.

bonds occur with metals that will not activate C—H bonds, use of Cp*Fe(P(OCH$_2$)$_3$CEt)$_2$R complexes is promising because of the demonstrated ability of the related Cp*Fe(CO)(NCMe)Ph to activate C—H bonds.[51] These studies establish the ability of d^6 complexes to mediate O atom insertion into M—R bonds. Importantly, they also point the way to new ligand motifs that avoid (1) C—C coupling products and (2) ligand oxidation.

EXPERIMENTAL SECTION

General Methods. Unless otherwise noted, all synthetic procedures were performed under anaerobic conditions in a nitrogen-filled glovebox or by using standard Schlenk techniques. Glovebox purity was maintained by periodic nitrogen purges and was monitored by an oxygen analyzer (O$_2$ < 15 ppm for all reactions). Tetrahydrofuran was dried by distillation from sodium/benzophenone. Diethyl ether was distilled over CaH$_2$. THF-d_8, CD$_3$CN, and D$_2$O were used as received and stored under a N$_2$ atmosphere over 4 Å molecular sieves (except water). ^{1}H NMR spectra were recorded on a Varian Mercury 300 MHz, Varian Inova 500 MHz, or Bruker 800 MHz spectrometer. ^{13}C NMR spectra were recorded using a Varian Mercury 300 MHz (operating frequency 75 MHz), Varian Inova 500 MHz (operating frequency 125 MHz), or Bruker 800 MHz (operating frequency 201 MHz) spectrometer. ^{31}P NMR spectra were recorded using a Varian Mercury 300 MHz (operating frequency 121 MHz) referenced against an external standard of H$_3$PO$_4$ (δ = 0). All ^{1}H and ^{13}C{^{1}H} spectra are referenced against residual proton signals (^{1}H NMR) or the ^{13}C signals of the deuterated solvents (^{13}C{^{1}H} NMR). GC/MS was performed using a Shimadzu GCMS-QP2010 Plus system with a 30 m × 0.25 mm RTx-Qbond column with 8 μm thickness using electron impact ionization. Photolysis experiments were performed using UV—vis radiation generated by a 450 W power supply (model #l7830, Ace Glass, Inc.) equipped with a water-cooled 450 W 5 in. arc IMMER UV—vis lamp (model #7825-34, Ace Glass, Inc.). All other reagents were used as purchased from commercial sources. Elemental analyses were performed by Atlantic Microlabs, Inc. [(TMEDA)FeCl$_2$]$_n$ (n = 1, 2) and Cp*Fe(CO)(NCMe)Ph (**1**) was prepared according to the literature procedure.[51,59]

Reaction of Cp*Fe(CO)(NCMe)Ph (1) with Oxidants. A representative experiment is described. Complex **1** (3.5 mg, 10 μmol) and pyridine *N*-oxide (2.9 mg, 30 μmol) were dissolved in 400 μL of THF-d_8 in an NMR tube. The reaction mixture was placed in an oil bath at 60 °C. The reaction was periodically removed from the oil bath and analyzed by ^{1}H NMR spectroscopy. D$_2$O (2 μL) was added to the reaction mixture, and the products were analyzed by ^{1}H NMR spectroscopy and/or GC-MS.

Cp*Fe(P(OCH$_2$)$_3$CEt)$_2$Cl (2). THF (50 mL) was cooled in a glovebox freezer at −30 °C for 30 min. After the cooling time period, the solution was added to a mixture of Cp*Li (1.01 g, 7.1 mmol), [(TMEDA)FeCl$_2$]$_n$ (n = 1, 2) (1.10 g, 4.53 mmol), and P(OCH$_2$)$_3$CEt (2.01 g, 12.3 mmol) in a round-bottom flask. The mixture was stirred and allowed to warm to room temperature over a period of approximately 30 min. The red-brown mixture was eluted through silica gel on a fine-porosity frit using THF. A red-brown band was collected, and most of the solvent was removed under vacuum. Hexanes (50 mL) were added to form a precipitate. The red-brown solid was collected via vacuum filtration, washed with hexanes, and dried under vacuum (1.79 g, 70% yield). ^{1}H NMR (300 MHz, THF-d_8): δ 4.17 (12H, s, P(OCH_2)$_3$CCH$_2$CH$_3$), 1.51 (15H, s, C$_5$(CH_3)$_5$), 1.20 (4H, q, $^3J_{HH}$ = 8 Hz, P(OCH$_2$)$_3$CCH_2CH$_3$), 0.82 (6H, t, $^3J_{HH}$ = 8 Hz, P(OCH$_2$)$_3$CCH$_2$CH_3). ^{13}C NMR (201 MHz, CD$_3$CN): δ 88.7 (P(OCH$_2$)$_3$CCH$_2$CH$_3$), 74.4 (C$_5$(CH$_3$)$_5$), 35.5 (P(OCH$_2$)$_3$CCH$_2$CH$_3$), 23.7 (P(OCH$_2$)$_3$CCH$_2$CH$_3$), 9.3 (C$_5$(CH$_3$)$_5$), 7.0 (P(OCH$_2$)$_3$CCH$_2$CH$_3$). ^{31}P NMR (121 MHz, CD$_3$CN): δ 163.8 (s).

Cp*Fe(P(OCH$_2$)$_3$CEt)$_2$Ph (3). Complex **2** (1.02 g, 1.80 mmol) was dissolved in THF (50 mL) in a Schlenk flask. The solution was then cooled in a 2-propanol/dry ice bath. A diethyl ether solution of PhLi (1.8 M, 2.2 mL, 4.0 mmol) was added to the solution of **2** with stirring. Upon addition of PhLi, the mixture turned to yellow from red-brown. The mixture was allowed to warm to room temperature. In a glovebox, the solution was eluted through silica gel using THF. A yellow band was collected, and most of the solvent was removed under vacuum. Hexanes (50 mL) were added to form a precipitate. The yellow solid was collected via filtration, washed with hexanes, and dried under vacuum (0.71 g, 65% yield). Single crystals suitable for X-ray diffraction were grown by slow diffusion of pentane into a THF solution of **3**. ^{1}H NMR (800 MHz, CD$_3$CN): δ 7.56 (2H, d, $^3J_{HH}$ = 7 Hz, phenyl *ortho*), 6.60 (2H, t, $^3J_{HH}$ = 7 Hz, phenyl *meta*), 6.60 (1H, t, $^3J_{HH}$ = 7 Hz, phenyl *para*), 4.07 (12H, s, P(OCH_2)$_3$CCH$_2$CH$_3$), 1.42 (15H, s, C$_5$(CH_3)$_5$), 1.15 (4H, q, $^3J_{HH}$ = 8 Hz, P(OCH$_2$)$_3$CCH_2CH$_3$), 0.77 (6H, t, $^3J_{HH}$ = 8 Hz, P(OCH$_2$)$_3$CCH$_2$CH_3). ^{13}C NMR (201 MHz, CD$_3$CN): δ 171.2 (*ipso* Ph, t, $^2J_{PC}$ = 34 Hz), 146.9, 125.2, 119.9 (Ph), 91.0 (P(OCH$_2$)$_3$CCH$_2$CH$_3$), 74.3 (C$_5$(CH$_3$)$_5$), 35.5 (P(OCH$_2$)$_3$CCH$_2$CH$_3$, t, $^3J_{PC}$ = 15 Hz), 24.0 (P(OCH$_2$)$_3$CCH$_2$CH$_3$), 10.0 (C$_5$(CH$_3$)$_5$), 7.3 (P(OCH$_2$)$_3$CCH$_2$CH$_3$). ^{31}P NMR (121 MHz, CD$_3$CN): δ 167.3 (s). Anal. Calcd for C$_{28}$H$_{42}$O$_6$P$_2$Fe: C 56.78, H 7.15. Found: C 56.88, H 7.20.

Cp*Fe(P(OCH$_2$)$_3$CEt)$_2$Me (5). Complex **5** was made by the same procedure as **3** but using a MeLi solution instead of a PhLi solution (65% isolated yield). ^{1}H NMR (300 MHz, CD$_3$CN): δ 4.02 (12H, s, P(OCH_2)$_3$CCH$_2$CH$_3$), 1.53 (15H, s, C$_5$(CH_3)$_5$), 1.13 (4H, q, $^3J_{HH}$ = 8 Hz, P(OCH$_2$)$_3$CCH_2CH$_3$), 0.76 (6H, t, $^3J_{HH}$ = 8 Hz, P(OCH$_2$)$_3$CCH$_2$CH_3), −0.96 (3H, t, $^3J_{PH}$ = 6 Hz, CH_3). ^{13}C NMR (201 MHz, CD$_3$CN): δ 89.0 (P(OCH$_2$)$_3$CCH$_2$CH$_3$), 74.3 (C$_5$(CH$_3$)$_5$), 35.3 (P(OCH$_2$)$_3$CCH$_2$CH$_3$, t, $^3J_{PC}$ = 15 Hz), 24.3 (P(OCH$_2$)$_3$CCH$_2$CH$_3$), 9.8 (C$_5$(CH$_3$)$_5$), 7.4 (P(OCH$_2$)$_3$CCH$_2$CH$_3$), −16.5 (CH$_3$, t, $^2J_{PC}$ = 30 Hz). ^{31}P NMR (121 MHz, CD$_3$CN): δ 167.5 (s). Anal. Calcd for C$_{23}$H$_{40}$O$_6$P$_2$Fe: C 52.21, H 7.60. Found: C 51.99, H 7.55.

Reaction of Cp*Fe(P(OCH$_2$)$_3$CEt)$_2$Ph (3) with Me$_3$NO. Complex **3** (3 mg, 5 μmol) and Me$_3$NO (2 mg, 25 μmol) were mixed in ~400 μL of THF-d_8 in an NMR tube under ambient light. The reaction was periodically analyzed by ^{1}H NMR spectroscopy. The reaction was complete in 4 days. D$_2$O (2 μL) was added to the reaction mixture, and the products were analyzed by ^{1}H NMR spectroscopy and GC-MS.

Reaction of Cp*Fe(P(OCH$_2$)$_3$CEt)$_2$Ph (3) with Me$_3$NO under Photolysis. Complex **3** (3 mg, 5 μmol) and Me$_3$NO (2 mg, 25 μmol) were mixed in ~400 μL of THF-d_8 in an NMR tube. The solution was placed in a photolysis cabinet with a Hg vapor lamp. The reaction was complete within 2 h (the products were analyzed by ^{1}H NMR spectroscopy).

Attempted Catalytic Oxidation of Benzene by Cp*Fe(P(OCH$_2$)$_3$CEt)$_2$Ph (3) with Me$_3$NO. Complex **3** (3 mg, 5 μmol) and Me$_3$NO (2 mg, 25 μmol) were mixed in ~400 μL of THF-d_8 in an

NMR tube. Benzene (2 μL, 22 μmol) and 1,4-cyclohexadiene (2 μL, 21 μmol) were added to the solution. $Me_3SiSiMe_3$ (~1 μL) was added as an internal standard for ^1H NMR spectroscopy. The solution was placed in a photolysis cabinet with a Hg vapor lamp. The reaction was complete within 20 min (the products were analyzed by ^1H NMR spectroscopy).

Reaction of $Cp^*Fe(P(OCH_2)_3CEt)_2Ph$ (3) with O_2. Complex **3** (3.0 mg, 5.0 μmol) was dissolved in 400 μL of THF-d_8. The reaction mixture was opened to air under ambient light for 1 day and periodically monitored by ^1H NMR spectroscopy. The products were analyzed by ^1H and ^{13}C NMR spectroscopy and GC-MS.

Reaction of $Cp^*Fe(P(OCH_2)_3CEt)_2Ph$ (3) with Oxidants. A representative experiment is described. Complex **3** (6.0 mg 10.1 μmol) and pyridine *N*-oxide (4.8 mg 50.0 μmol) were dissolved in 400 μL of THF-d_8 in an NMR tube. The reaction mixture was placed in an oil bath at 70 °C. The reaction was periodically removed from the oil bath and analyzed by ^1H NMR spectroscopy. Brønsted acid (D_2O or HCl) was added to the reaction mixture, and the products were analyzed by ^1H NMR spectroscopy and/or GC-MS.

Kinetics for Reaction of $Cp^*Fe(P(OCH_2)_3CEt)_2Ph$ (3) with PMe_3. A representative kinetic experiment is described. Complex **3** (6.0 mg 10 μmol) and 5 μL of PMe_3 (3.6 mg, 50 μmol) were dissolved in 400 μL of THF-d_8. The compound $OPPh_3$ (~3 mg) was added as an internal standard for ^{31}P NMR spectroscopy. The reaction mixture was placed in the photolysis cabinet 40 cm away from the Hg vapor lamp (the distance is important). A ^{31}P NMR spectrum was acquired every 10 min. Integration of the ^{31}P NMR peak of complex **3** gave the variation in concentration. Similar reactions were set up for 10.0, 15.0, and 20.0 μL of PMe_3. To ensure reproducibility, every concentration was repeated in triplicate.

Kinetics for Reaction of $Cp^*Fe(P(OCH_2)_3CEt)_2Ph$ (3) with Me_3NO. A representative kinetic experiment is described. Complex **3** (0.3 mg, 0.5 μmol) and Me_3NO (3.0 mg, 40 μmol) were dissolved in 500 μL of THF-d_8 (Me_3NO is partially dissolved and saturated in the solution). The compound $Me_3SiSiMe_3$ (~1 μL) was added as an internal standard for ^1H NMR spectroscopy. The reaction mixture was placed in the photolysis cabinet 40 cm away from the Hg vapor lamp. A ^1H NMR spectrum was acquired every 5 min for the first 30 min and every 10 min thereafter. Integration of the ^1H NMR spectra gave the variation in concentration of complex **3**, $P(OCH_2)_3CEt$, $PhOH\cdot ONMe_3$, and 1,2,3,4-tetramethylfulvene. To ensure reproducibility, each experiment was repeated in triplicate.

Kinetics for Reaction of $P(OCH_2)_3CEt$ with Me_3NO. A representative kinetic experiment is described. $P(OCH_2)_3CEt$ (0.3 mg, 0.5 μmol) was dissolved in 1.6 mL of THF-d_8. The compound $Me_3SiSiMe_3$ (3.0 μL) was added as an internal standard for ^1H NMR spectroscopy. Me_3NO (3.0 mg, 40 μmol) was added to a screw-cap tube. A 500 μL aliquot of the $P(OCH_2)_3CEt$ solution was transferred to the Me_3NO in the tube and timed as the start of the reaction. The tube was shaken for about 30 s to help dissolve the Me_3NO (Me_3NO is partially dissolved and saturated in the solution). The reaction mixture was then monitored by array ^1H NMR spectroscopy on a 500 MHz spectrometer at room temperature (20.4 °C). ^1H NMR spectra were acquired every 2 min for 120 min total. Integration of the ^1H NMR spectra gave the variation in concentration of $P(OCH_2)_3CEt$. To ensure reproducibility, each experiment was repeated in triplicate.

Computational Methods. Density functional theory within the Gaussian 09 package[60] was used for geometry optimization and vibrational frequency calculations. The hybrid meta-GGA functional wB97XD[61] was employed with a double-ζ basis set with pseudopotentials and added d functions for group elements (e.g., CEP-31G(d)).[62] This functional contains empirical dispersion terms and also long-range corrections. Tests with a larger, all-electron basis set—including diffuse functions on main group elements (B3LYP/6-31+G(d))—as well as Truhlar's M06[63] functional (M06/6-31+G(d)) did not yield significantly different calculated geometries or free energies. MECP calculations on full models of **3** were carried out at the wB97XD/6-31+G(d) level of theory. Calculations were carried out in the continuum SMD[64] solvation method with THF ($\varepsilon = 7.58$) being the solvent.

The energies quoted are free energies that were calculated at 298.15 K and 1 atm. The stationary points were defined as minima or transition states by the presence of 0 or 1 imaginary frequency, respectively, as obtained from the calculated energy Hessians. Various spin states were studied with only results for the lowest energy spin state reported.

■ ASSOCIATED CONTENT

Ⓢ Supporting Information

Kinetics plots, NMR spectra, GC/MS data, and computational details. This material is available free of charge via the Internet at http://pubs.acs.org.

■ AUTHOR INFORMATION

Corresponding Authors

*E-mail (T. B. Gunnoe): tbg7h@virginia.edu.
*E-mail (T. R. Cundari): t@unt.edu.

Notes

The authors declare no competing financial interest.

■ ACKNOWLEDGMENTS

The authors acknowledge Anna V. Sberegaeva and Prof. Andrei N. Vedernikov (University of Maryland) for preliminary experiments focused on aerobic oxidation. This work was solely supported as part of the Center for Catalytic Hydrocarbon Functionalization, an Energy Frontier Research Center funded by the U.S. Department of Energy, Office of Science, Office of Basic Energy Sciences, under Award No. DE-SC0001298. J.M. acknowledges Dr. Bradley McKeown for helpful discussions.

■ REFERENCES

(1) Crabtree, R. H. *J. Chem. Soc., Dalton Trans.* **2001**, 2437.
(2) Wittcoff, H. A.; Reuben, B. G.; Plotkin, J. S. *Industrial Organic Chemicals*, 2nd ed.; John Wiley & Sons, 2004.
(3) George, A. Olah, A. M. *Hydrocarbon Chemistry*, 2nd ed.; John Wiley & Sons, 2003.
(4) Conley, B. L.; Tenn, W. J.; Young, K. J. H.; Ganesh, S.; Meier, S.; Ziatdinov, V.; Mironov, O.; Oxgaard, J.; Gonzales, J.; Goddard, W. A.; Periana, R. A. In *Activation of Small Molecules*; Wiley-VCH Verlag GmbH & Co. KGaA, 2006; p 235.
(5) Goldberg, K. I.; Goldman, A. S. In *Activation and Functionalization of C-H Bonds*; American Chemical Society, 2004.
(6) Webb, J. R.; Bolaño, T.; Gunnoe, T. B. *ChemSusChem* **2011**, *4*, 37.
(7) Labinger, J. A.; Bercaw, J. E. *Nature* **2002**, *417*, 507.
(8) Labinger, J. A. *J. Mol. Catal. A: Chem.* **2004**, *220*, 27.
(9) Crabtree, R. H. *Chem. Rev.* **1985**, *85*, 245.
(10) Cavaliere, V. N.; Mindiola, D. J. *Chem. Sci.* **2012**, *3*, 3356.
(11) Sen, A. *Acc. Chem. Res.* **1998**, *31*, 550.
(12) Periana, R. A.; Taube, D. J.; Evitt, E. R.; Löffler, D. G.; Wentrcek, P. R.; Voss, G.; Masuda, T. *Science* **1993**, *259*, 340.
(13) Muehlhofer, M.; Strassner, T.; Herrmann, W. A. *Angew. Chem., Int. Ed.* **2002**, *41*, 1745.
(14) Shilov, A. E.; Shul'pin, G. B. *Chem. Rev.* **1997**, *97*, 2879.
(15) Shu, L.; Nesheim, J. C.; Kauffmann, K.; Münck, E.; Lipscomb, J. D.; Que, L., Jr. *Science* **1997**, *275*, 515.
(16) Liu, K. E.; Lippard, S. J. In *Advances in Inorganic Chemistry*; Sykes, A. G., Ed.; Academic Press, 1995; Vol. *42*, p 263.
(17) Wallar, B. J.; Lipscomb, J. D. *Chem. Rev.* **1996**, *96*, 2625.
(18) Groves, J. T.; McClusky, G. A. *J. Am. Chem. Soc.* **1976**, *98*, 859.
(19) Gunay, A.; Theopold, K. H. *Chem. Rev.* **2010**, *110*, 1060.
(20) Liu, W.; Huang, X.; Cheng, M.-J.; Nielsen, R. J.; Goddard, W. A.; Groves, J. T. *Science* **2012**, *337*, 1322.
(21) Chen, M. S.; White, M. C. *Science* **2007**, *318*, 783.

(22) Bigi, M. A.; Reed, S. A.; White, M. C. *J. Am. Chem. Soc.* **2012**, *134*, 9721.
(23) Zhou, M.; Balcells, D.; Parent, A. R.; Crabtree, R. H.; Eisenstein, O. *ACS Catal.* **2011**, *2*, 208.
(24) Qin, K.; Incarvito, C. D.; Rheingold, A. L.; Theopold, K. H. *J. Am. Chem. Soc.* **2002**, *124*, 14008.
(25) Lersch, M.; Tilset, M. *Chem. Rev.* **2005**, *105*, 2471.
(26) Arndtsen, B. A.; Bergman, R. G.; Mobley, T. A.; Peterson, T. H. *Acc. Chem. Res.* **1995**, *28*, 154.
(27) Bromberg, S. E.; Yang, H.; Asplund, M. C.; Lian, T.; McNamara, B. K.; Kotz, K. T.; Yeston, J. S.; Wilkens, M.; Frei, H.; Bergman, R. G.; Harris, C. B. *Science* **1997**, *278*, 260.
(28) Jones, W. D.; Feher, F. J. *Acc. Chem. Res.* **1989**, *22*, 91.
(29) Choi, G.; Morris, J.; Brennessel, W. W.; Jones, W. D. *J. Am. Chem. Soc.* **2012**, *134*, 9276.
(30) Webb, J. R.; Burgess, S. A.; Cundari, T. R.; Gunnoe, T. B. *Dalton Trans.* **2013**, *42*, 16646.
(31) Gunnoe, T. B. In *Physical Inorganic Chemistry: Reactions, Processes, and Applications*; Bacak, A., Ed.; Wiley-VCH, 2010; p 495.
(32) Vetter, A. J.; Flaschenriem, C.; Jones, W. D. *J. Am. Chem. Soc.* **2005**, *127*, 12315.
(33) Conley, B. L.; Ganesh, S. K.; Gonzales, J. M.; Tenn, W. J.; Young, K. J. H.; Oxgaard, J.; Goddard, W. A.; Periana, R. A. *J. Am. Chem. Soc.* **2006**, *128*, 9018.
(34) Bischof, S. M.; Cheng, M.-J.; Nielsen, R. J.; Gunnoe, T. B.; Goddard, W. A.; Periana, R. A. *Organometallics* **2011**, *30*, 2079.
(35) Gonzales, J. M.; Distasio, R.; Periana, R. A.; Goddard, W. A.; Oxgaard, J. *J. Am. Chem. Soc.* **2007**, *129*, 15794.
(36) Tenn, W. J.; Conley, B. L.; Hövelmann, C. H.; Ahlquist, M. r.; Nielsen, R. J.; Ess, D. H.; Oxgaard, J.; Bischof, S. M.; Goddard, W. A.; Periana, R. A. *J. Am. Chem. Soc.* **2009**, *131*, 2466.
(37) Feng, Y.; Lail, M.; Barakat, K. A.; Cundari, T. R.; Gunnoe, T. B.; Petersen, J. L. *J. Am. Chem. Soc.* **2005**, *127*, 14174.
(38) Tenn, W. J.; Young, K. J. H.; Bhalla, G.; Oxgaard, J.; Goddard, W. A.; Periana, R. A. *J. Am. Chem. Soc.* **2005**, *127*, 14172.
(39) Kloek, S. M.; Heinekey, D. M.; Goldberg, K. I. *Angew. Chem., Int. Ed.* **2007**, *46*, 4736.
(40) Bercaw, J. E.; Hazari, N.; Labinger, J. A. *Organometallics* **2009**, *28*, 5489.
(41) Feng, Y.; Lail, M.; Foley, N. A.; Gunnoe, T. B.; Barakat, K. A.; Cundari, T. R.; Petersen, J. L. *J. Am. Chem. Soc.* **2006**, *128*, 7982.
(42) Cundari, T. R.; Grimes, T. V.; Gunnoe, T. B. *J. Am. Chem. Soc.* **2007**, *129*, 13172.
(43) Van Asselt, A.; Trimmer, M. S.; Henling, L. M.; Bercaw, J. E. *J. Am. Chem. Soc.* **1988**, *110*, 8254.
(44) Brown, S. N.; Mayer, J. M. *J. Am. Chem. Soc.* **1996**, *118*, 12119.
(45) Kamaraj, K.; Bandyopadhyay, D. *Organometallics* **1999**, *18*, 438.
(46) Mei, J.; Carsch, K. M.; Freitag, C. R.; Gunnoe, T. B.; Cundari, T. R. *J. Am. Chem. Soc.* **2012**, *135*, 424.
(47) Pouy, M. J.; Milczek, E. M.; Figg, T. M.; Otten, B. M.; Prince, B. M.; Gunnoe, T. B.; Cundari, T. R.; Groves, J. T. *J. Am. Chem. Soc.* **2012**, *134*, 12920.
(48) Ni, C.; Power, P. P. *Chem. Commun.* **2009**, 5543.
(49) Matsunaga, P. T.; Hillhouse, G. L.; Rheingold, A. L. *J. Am. Chem. Soc.* **1993**, *115*, 2075.
(50) Alsters, P. L.; Boersma, J.; van Koten, G. *Organometallics* **1993**, *12*, 1629.
(51) Kalman, S. E.; Petit, A.; Gunnoe, T. B.; Ess, D. H.; Cundari, T. R.; Sabat, M. *Organometallics* **2013**, *32*, 1797.
(52) Pardue, D. B.; Mei, J.; Cundari, T. R.; Gunnoe, T. B. *Inorg. Chem.* **2014**, *53*, 2968.
(53) Tilset, M.; Fjeldahl, I.; Hamon, J.-R.; Hamon, P.; Toupet, L.; Saillard, J.-Y.; Costuas, K.; Haynes, A. *J. Am. Chem. Soc.* **2001**, *123*, 9984.
(54) Mendenhall, G. D.; Kessick, R. F.; Dobrzelewski, M. *J. Photochem.* **1984**, *25*, 227.
(55) Beckwith, A. L. J.; Bowry, V. W.; Ingold, K. U. *J. Am. Chem. Soc.* **1992**, *114*, 4983.
(56) Harvey, J. N.; Aschi, M.; Schwarz, H.; Koch, W. *Theor. Chem. Acc.* **1998**, *99*, 95.
(57) Harvey, J. N.; Aschi, M. *Phys. Chem. Chem. Phys.* **1999**, *1*, 5555.
(58) Sako, M.; Shimada, K.; Hirota, K.; Maki, Y. *J. Am. Chem. Soc.* **1986**, *108*, 6039.
(59) Davies, S. C.; Hughes, D. L.; Leigh, G. J.; Sanders, J. R.; de Souza, J. S. *J. Chem. Soc., Dalton Trans.* **1997**, 1981.
(60) Frisch, M. J.,; Trucks, G. W.; Schlegel, H. B.; Scuseria, G. E.; Robb, M. A.; Cheeseman, J. R.; Scalmani, G.; Barone, V.; Mennucci, B.; Petersson, G. A.; Nakatsuji, H.; Caricato, M.; Li, X.; Hratchian, H. P.; Izmaylov, A. F.; Bloino, J.; Zheng, G.; Sonnenberg, J. L.; Hada, M.; Ehara, M.; Toyota, K.; Fukuda, R.; Hasegawa, J.; Ishida, M.; Nakajima, T.; Honda, Y.; Kitao, O.; Nakai, H.; Vreven, T.; Montgomery, J. A., Jr.; Peralta, J. E.; Ogliaro, F.; Bearpark, M.; Heyd, J. J.; Brothers, E.; Kudin, K. N.; Staroverov, V. N.; Kobayashi, R.; J. R. Normand, K.; Rendell, A.; Burant, J. C.; Iyengar, S. S.; Tomasi, J.; Cossi, M.; Rega, N.; Millam, N. J.; Klene, M.; Knox, J. E.; Cross, J. B.; Bakken, V.; Adamo, C.; Jaramillo, J.; Gomperts, R.; Stratmann, R. E.; Yazyev, O.; Austin, A. J.; Cammi, R.; Pomelli, C.; Ochterski, J. W.; Martin, R. L.; Morokuma, K.; Zakrzewski, V. G.; Voth, G. A.; Salvador, P.; Dannenberg, J. J.; Dapprich, S.; Daniels, A. D.; Ö. Farkas, Foresman, J. B.; Ortiz, J. V.; Cioslowski, J.; Fox, D. J. *Gaussian*, Revision B.01 ed.; Gaussian Inc: Wallingford, CT, 2009.
(61) Grimme, S. *J. Comput. Chem.* **2006**, *27*, 1787.
(62) Stevens, W. J.; Krauss, M.; Basch, H.; Jasien, P. G. *Can. J. Chem.* **1992**, *70*, 612.
(63) Zhao, Y.; Truhlar, D. *Theor. Chem. Acc.* **2008**, *120*, 215.
(64) Marenich, A. V.; Cramer, C. J.; Truhlar, D. G. *J. Phys. Chem. B* **2009**, *113*, 6378.